Climate variability

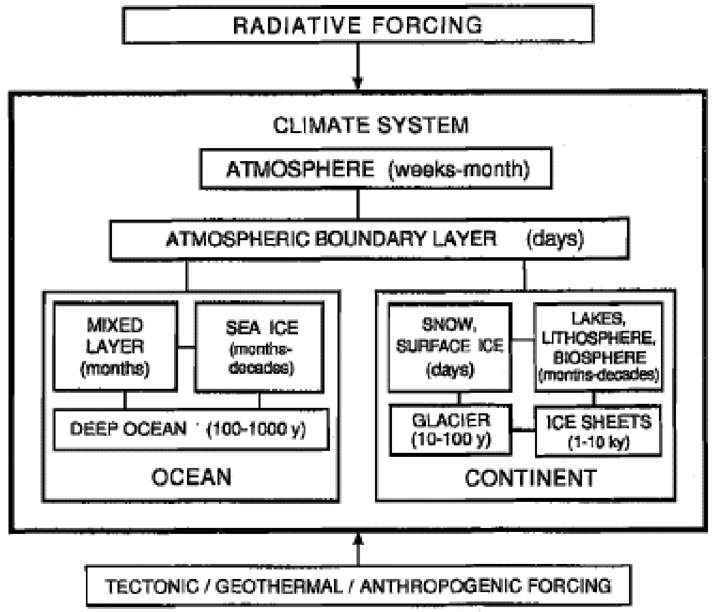

Figure 1-1 Schematic representation of the component domains of the internal climate system, showing their typical response time constants, and main sources of forcing.

Saltzman (2002)

Readings

(i) Saltzman, B., 2002, Dynamical Paleoclimatology: Generalized Theory of Global Climate Change. Academic Press, San Diego, 354 pp. (ii) Crowley, T. and North, G., 1991: Paleoclimatology. Oxford University Press, Oxford, 339 pp. (ii) Ruddimann, W.F., 2000: Earth's Climate: Past and Future. W.H: Freeman and Company, New York, 465 pp. (iii) Burroughs, W.J., 1992: Weather Cycles: Real or Imaginary? Cambridge University Press, Cambridge, 207 pp. (iv) Philander, S.G., 1990: El Niño, La Niña, and the Southern Oscillation. Academic Press, London, 289 pp. ; (v) Philander, S.G.H., 1983, El Niño Southern Oscillation phenomena. Nature, 302, 295-301. (vi) Latif, M., 2004: Klima. Fischer Verlag, Frankfurt am Main, 128 S.

Variability

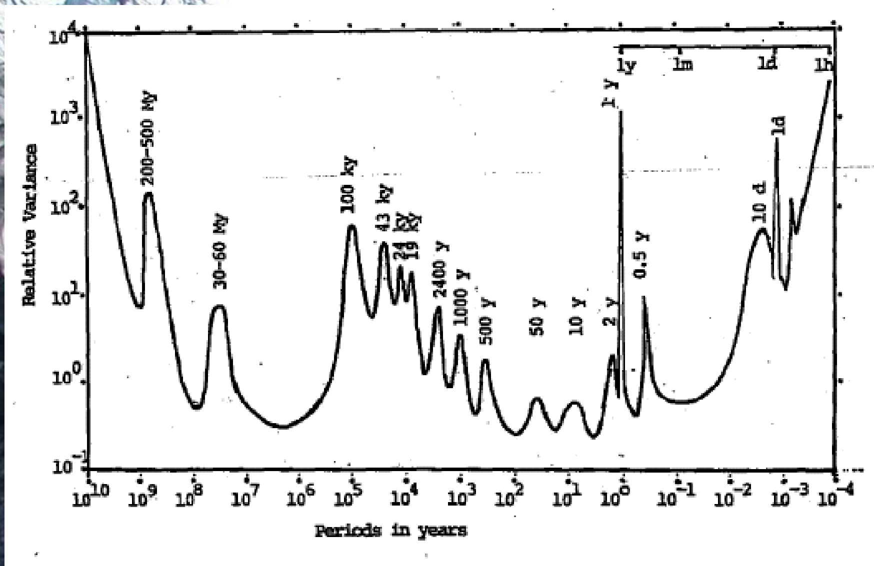

Variability of the thermal state of the atmosphere.
After Ohmura (2006)

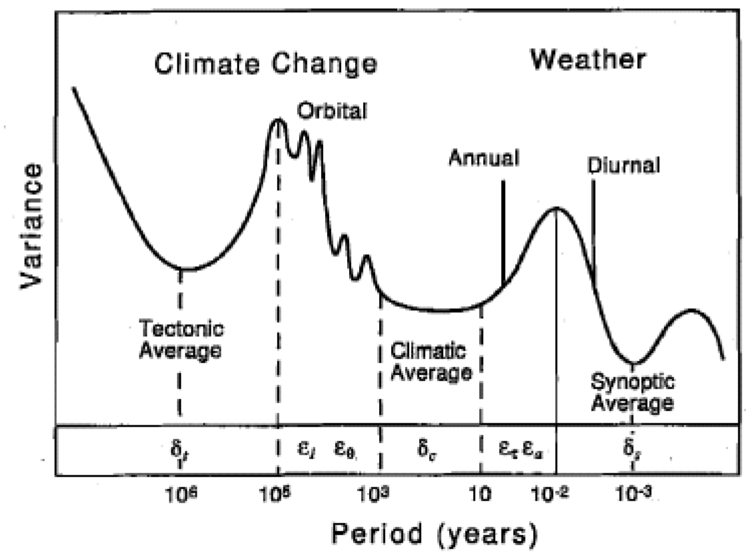

Figure 1-2 Hypothetical, highly idealized, spectrum of atmospheric thermal variance at a midlatitude point over the age of the Earth. δ_s, δ_c, and δ_t denote the synoptic, climatic, and tectonic averaging intervals, respectively, and ε_a, ε_τ, ε_θ, and ε_I denote the approximate response times for the atmosphere, oceanic mixed layer, deep ocean, and ice sheets, respectively, as will be discussed in Section 4.3.

Saltzman (2002)

Time scales

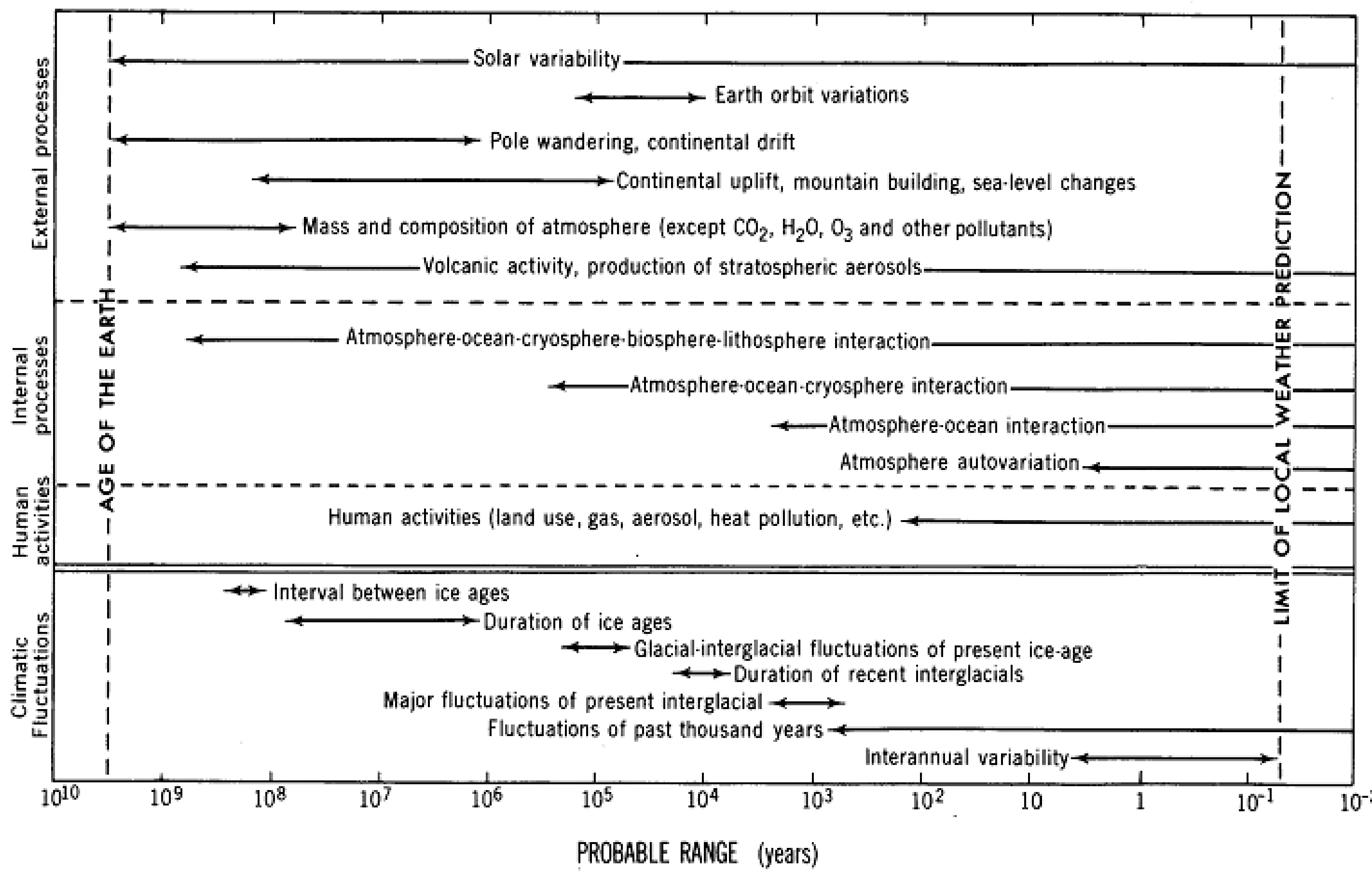

Peixoto, J. and Oort, A., 1992: Physics of Climate. American Institute of Physics, New York, 520 pp.

The ice-age problem

The ice-age problem

The ice age problem can be visualized with reference to the following figures (from Saltzman, 2002).

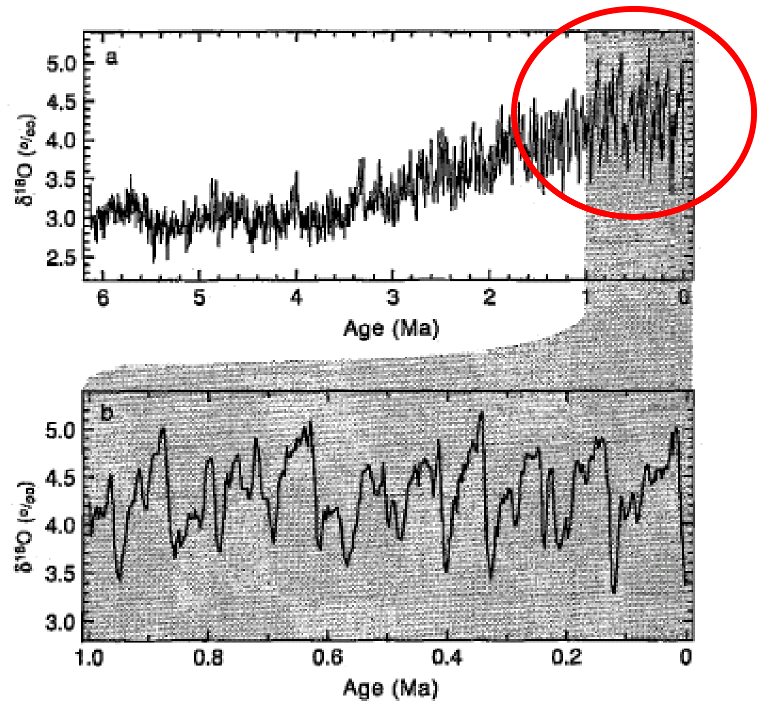

Figure 1-4 (a) δ^{18}O-Derived estimates of global ice mass variability over 6 My; (b) a more detailed view of the past 1 My. After Shackleton (1999).

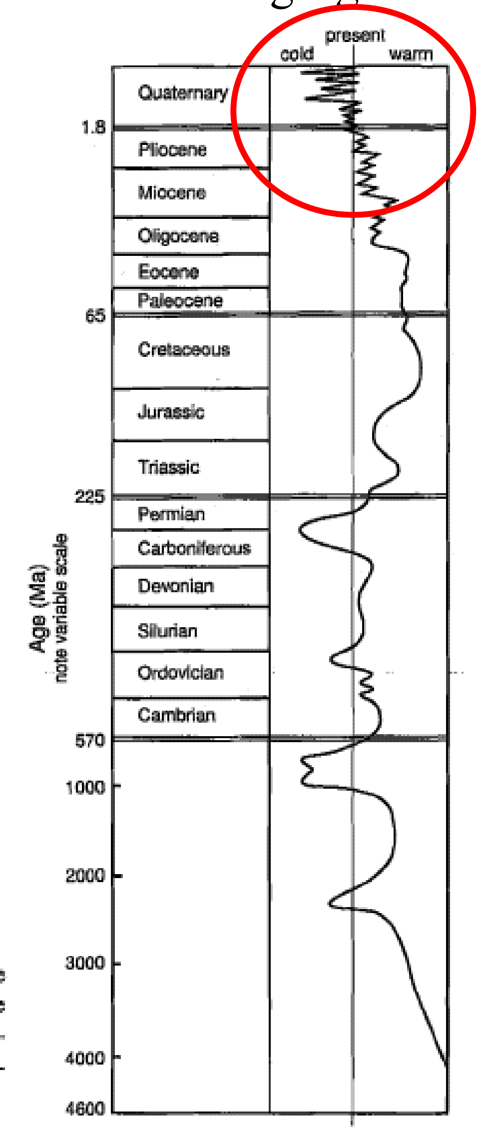

Figure 1-3 Idealized representation of the variations of mean global temperature over the age of the Earth based on geologic proxy evidence. Coldest periods are associated with large-scale glaciation. After Frakes (1979).

Earth's face

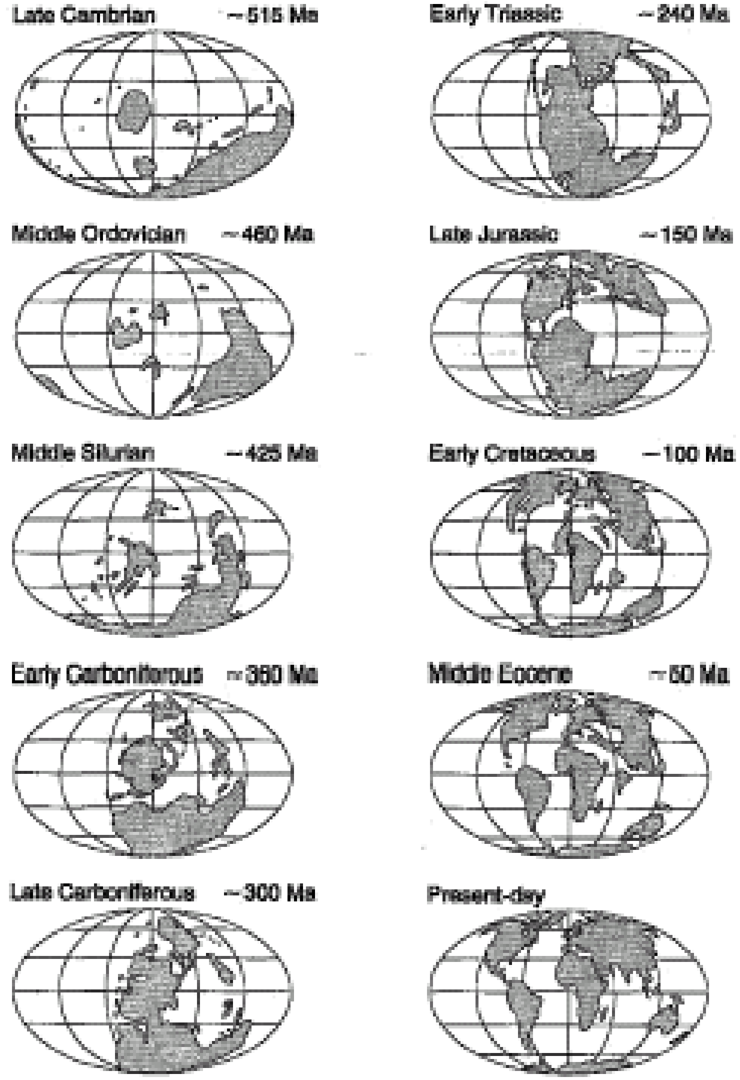

Figure 3-1 Evolution of the continent–ocean distribution over the past 500 My. After Scotese (1997).

Saltzman (2002).

A proxy for the global ice volume

The oceanic $\delta^{18}O$ [‰] records can considered a proxy for the record of the global ice volume. The variable $\delta^{18}O$ is defined as:

$$\delta^{18}O = \frac{R_{sample} - R_{standard}}{R_{standard}} \cdot 1000$$

where R is the isotopic mass ratio, in this case $R = {}^{18}O/{}^{16}O$, and the standard is provided by the U.S. National Bureau of Standards. Changes in $\delta^{18}O$ are related to the isotope fractionation occurring with the evaporation of water vapor from the ocean, the atmospheric transport toward high latitudes and the formation of precipitation.

Formulation of the ice-age problem

Returning to the ice-age problem, we can put down the following main questions:

- How do we explain the onset of glaciations at ~ 2 Myr before present?
- How do we explain the onset of a near 100-kyr quasi cyclic oscillation at ~ 1 Myr before present?
- How do we explain periodicities of near 20 and 40 kyr?
- Are the periodicities at near 20, 40 and 100 kyr all forced by changes in the orbital parameters?

Long-term climatic variations in insolation: Milankovitch theory

Let us fist have a look at the variation of the orbital elements (Berger, 1991). The three key elements in the orbital geometry are:

- the eccentricity, e;
- the obliquity of the earth's rotation axis relativ to the ecliptic plane, ε;
- the longitude of the perihelion, ω. The variability of e and ω induces the so-called axial precession.

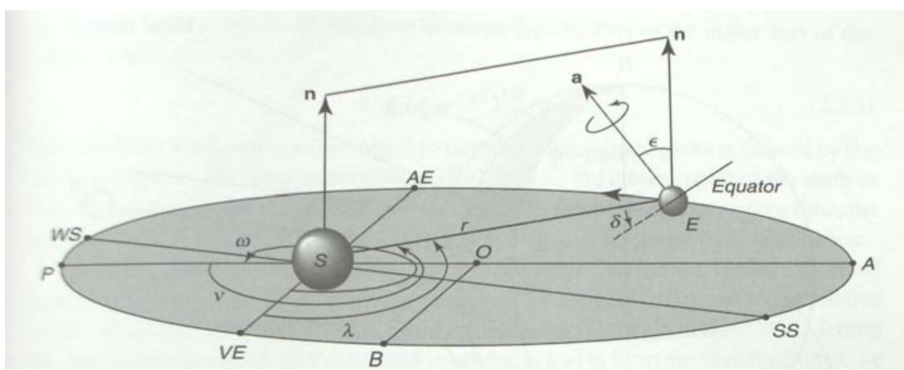

After Liou (2002)

Berger A. and Loutre M.F., 1991: Insolation values for the climate of the last 10 million years. Quaternary Sciences Review, Vol. 10 No. 4, pp. 297-317, 1991.

Long-term climatic variations in insolation (2)

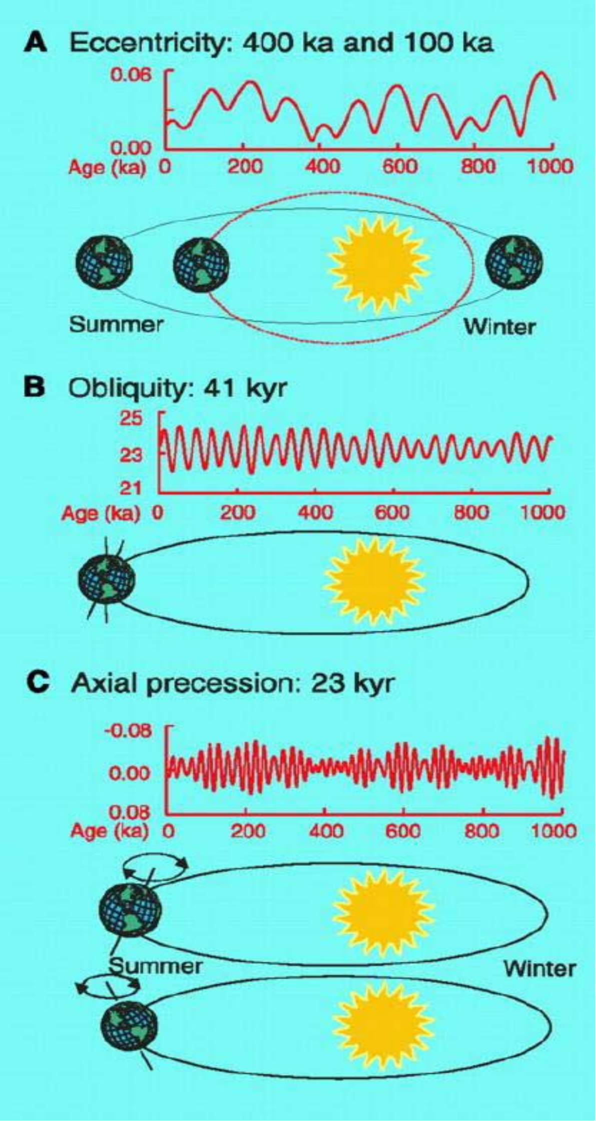

Long-term climatic variations in insolation (3)

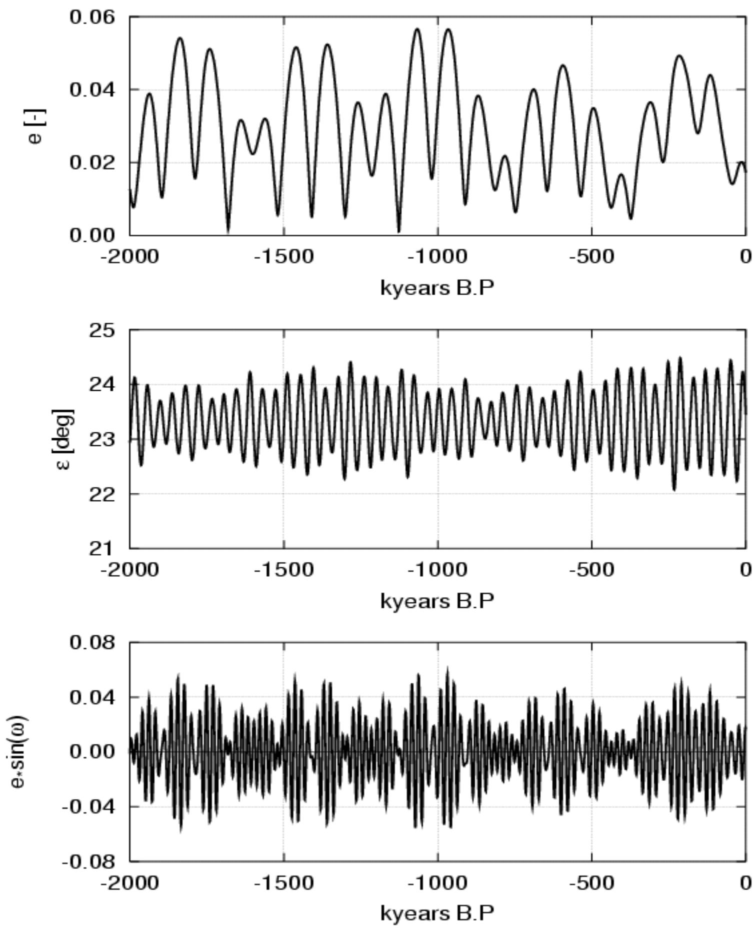

eccentricity
periodicity (P) of 100 and 413 kyr

obliquity
P of 41 kyr

precession, e·sin(ω),
P of 23 and 18 kyr

Data calculated according to Berger and Loutre (1991).

Long-term climatic variations in insolation (4)

Changes in the orbital elements give rise to changes in the insolation, which are particularly pronounced at high latitudes. Milankovitch (1941) postulated that variations in the summer insolation of the NH high latitudes (~ 65 ^{o}N) alter summer melt and affect therefore the mass balance of polar ice sheets.

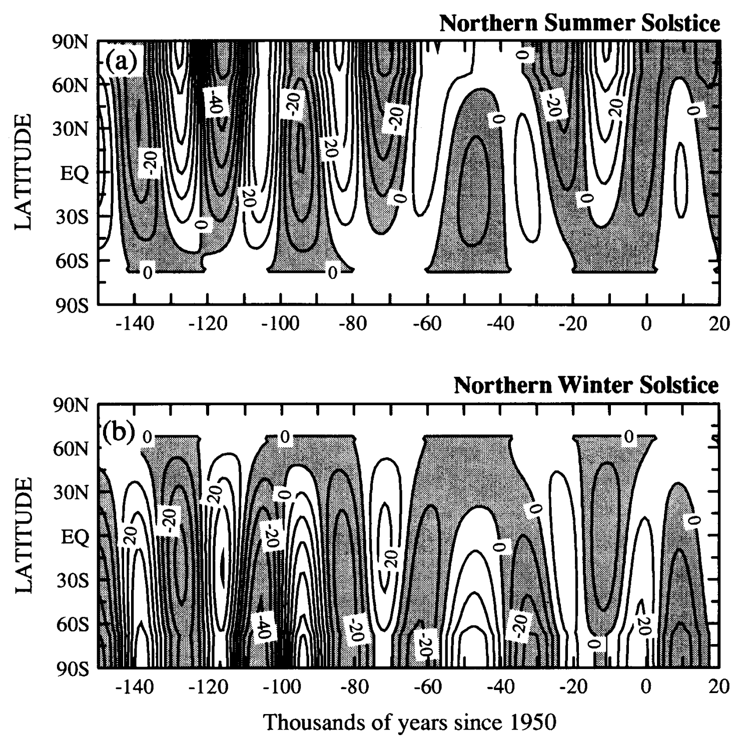

Hartmann (1994)

Milankovitch, M., 1941: Kanon der Erdbestrahlung und seine Anwendung auf das Eiszeitproblem. Beograd, Königliche Serbische Akademie.

Hartmann, D.L., 1994: Global Physical Climatology. Academic Press, San Diego.

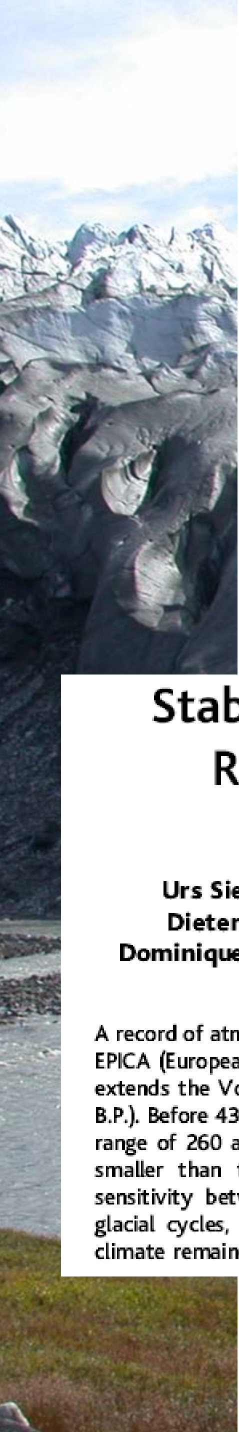

Ice-core records

Climate and atmospheric history of the past 420,000 years from the Vostok ice core, Antarctica

J. R. Petit*, J. Jouzel†, D. Raynaud*, N. I. Barkov‡, J.-M. Barnola*, I. Basile*, M. Bender§, J. Chappellaz*, M. Davis||, G. Delaygue†, M. Delmotte*, V. M. Kotlyakov¶, M. Legrand*, V. Y. Lipenkov‡, C. Lorius*, L. Pépin*, C. Ritz*, E. Saltzman|| & M. Stievenard†

* *Laboratoire de Glaciologie et Géophysique de l'Environnement, CNRS, BP96, 38402, Saint Martin d'Hères Cedex, France*
† *Laboratoire des Sciences du Climat et de l'Environnement (UMR CEA/CNRS 1572), L'Orme des Merisiers, Bât. 709, CEA Saclay, 91191 Gif-sur-Yvette Cedex, France*
‡ *Arctic and Antarctic Research Institute, Beringa Street 38, 199397, St Petersburg, Russia*
§ *Department of Geosciences, Princeton University, Princeton, New Jersey 08544-1003, USA*
|| *Rosenstiel School of Marine and Atmospheric Science, University of Miami, 4600 Rickenbacker Causeway, Miami, Florida 33149, USA*
¶ *Institute of Geography, Staromonetny, per 29, 109017, Moscow, Russia*

Nature, 1999, 399, 429-436

Stable Carbon Cycle–Climate Relationship During the Late Pleistocene

Urs Siegenthaler,[1] Thomas F. Stocker,[1*] Eric Monnin,[1] Dieter Lüthi,[1] Jakob Schwander,[1] Bernhard Stauffer,[1] Dominique Raynaud,[2] Jean-Marc Barnola,[2] Hubertus Fischer,[3] Valérie Masson-Delmotte,[4] Jean Jouzel[4]

A record of atmospheric carbon dioxide (CO_2) concentrations measured on the EPICA (European Project for Ice Coring in Antarctica) Dome Concordia ice core extends the Vostok CO_2 record back to 650,000 years before the present (yr B.P.). Before 430,000 yr B.P., partial pressure of atmospheric CO_2 lies within the range of 260 and 180 parts per million by volume. This range is almost 30% smaller than that of the last four glacial cycles; however, the apparent sensitivity between deuterium and CO_2 remains stable throughout the six glacial cycles, suggesting that the relationship between CO_2 and Antarctic climate remained rather constant over this interval.

Atmospheric Methane and Nitrous Oxide of the Late Pleistocene from Antarctic Ice Cores

Renato Spahni,[1] Jérôme Chappellaz,[2] Thomas F. Stocker,[1*] Laetitia Loulergue,[2] Gregor Hausammann,[1] Kenji Kawamura,[1†] Jacqueline Flückiger,[1‡] Jakob Schwander,[1] Dominique Raynaud,[2] Valérie Masson-Delmotte,[3] Jean Jouzel[3]

The European Project for Ice Coring in Antarctica Dome C ice core enables us to extend existing records of atmospheric methane (CH_4) and nitrous oxide (N_2O) back to 650,000 years before the present. A combined record of CH_4 measured along the Dome C and the Vostok ice cores demonstrates, within the resolution of our measurements, that preindustrial concentrations over Antarctica have not exceeded 773 ± 15 ppbv (parts per billion by volume) during the past 650,000 years. Before 420,000 years ago, when interglacials were cooler, maximum CH_4 concentrations were only about 600 ppbv, similar to lower Holocene values. In contrast, the N_2O record shows maximum concentrations of 278 ± 7 ppbv, slightly higher than early Holocene values.

Science, 2005, 310, 1313-1317

Variability in ice-core records

The problem of dating

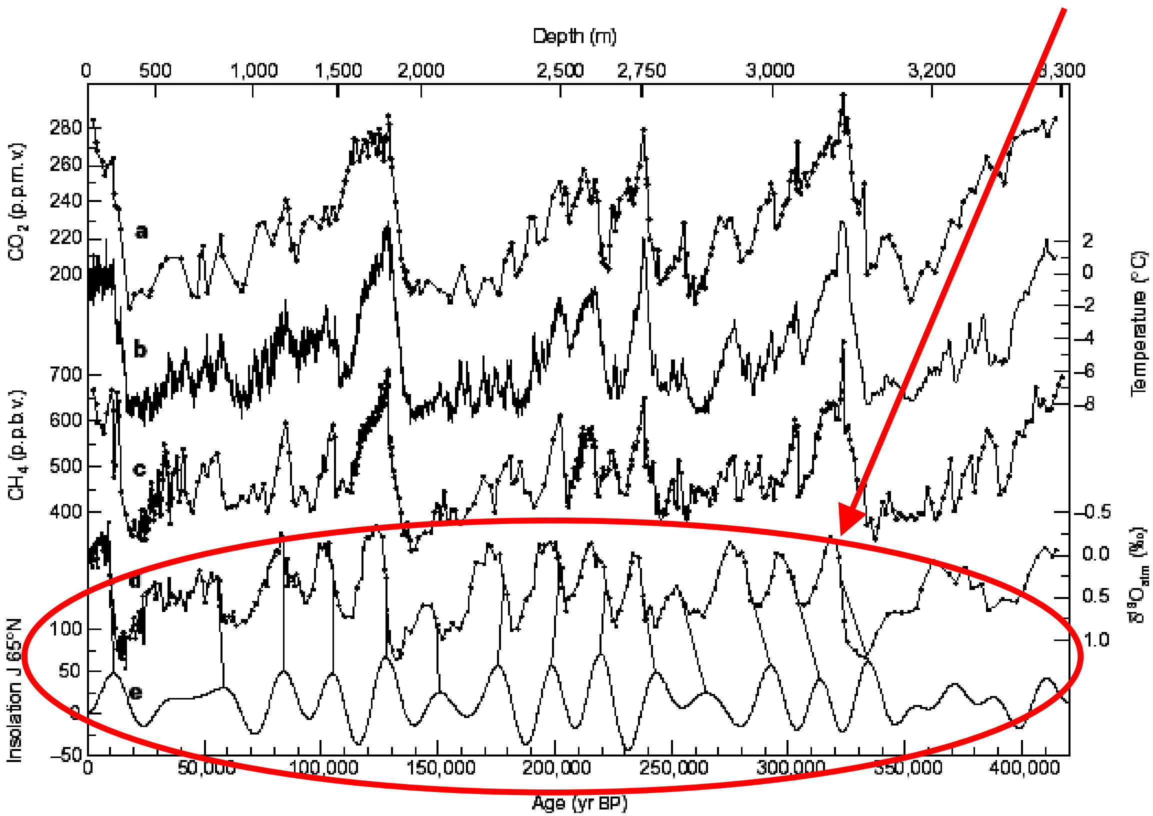

Figure 3 Vostok time series and insolation. Series with respect to time (GT4 timescale for ice on the lower axis, with indication of corresponding depths on the top axis) of: **a**, CO_2; **b**, isotopic temperature of the atmosphere (see text); **c**, CH_4; **d**, $\delta^{18}O_{atm}$; and **e**, mid-June insolation at 65°N (in Wm^{-2}) (ref. 3). CO_2 and CH_4 measurements have been performed using the methods and analytical procedures previously described[5,9]. However, the CO_2 measuring system has been slightly modified in order to increase the sensitivity of the CO_2 detection. The thermal conductivity chromatographic detector has been replaced by a flame ionization detector which measures CO_2 after its transformation into CH_4. The mean resolution of the CO_2 (CH_4) profile is about 1,500 (950) years. It goes up to about 6,000 years for CO_2 in the fractured zones and in the bottom part of the record, whereas the CH_4 time resolution ranges between a few tens of years to 4,500 years. The overall accuracy for CH_4 and CO_2 measurements are ±20 p.p.b.v. and 2–3 p.p.m.v., respectively. No gravitational correction has been applied.

Petit, J.R. et al. (1999)

Variability ice-core records (2)

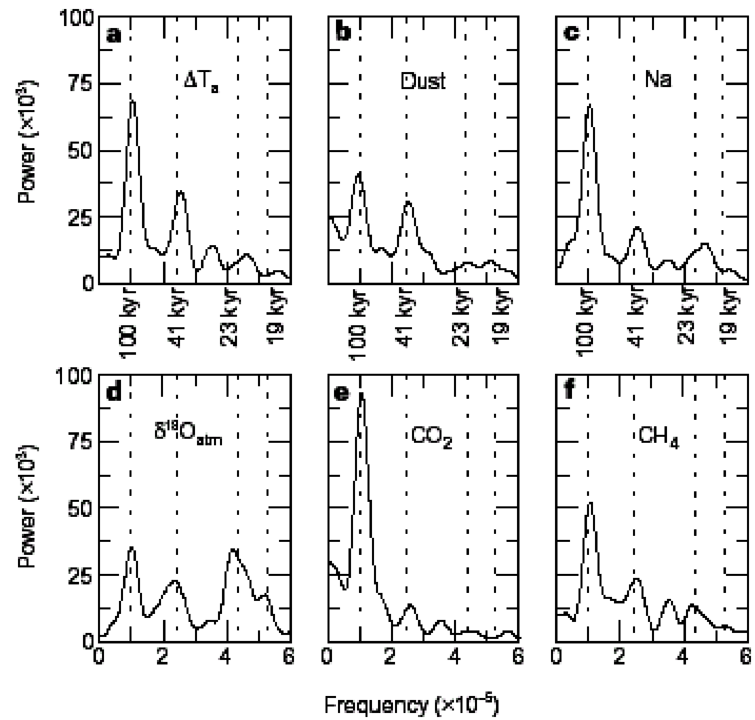

Figure 4 Spectral properties of the Vostok time series. Frequency distribution (in cycles yr^{-1}) of the normalized variance power spectrum (arbitrary units). Spectral analysis was done using the Blackman-Tukey method (calculations were performed with the Analyseries software[47]): **a**, isotopic temperature; **b**, dust; **c**, sodium; **d**, $\delta^{18}O_{atm}$; **e**, CO_2; and **f**, CH_4. Vertical lines correspond to periodicities of 100, 41, 23 and 19 kyr.

Petit, J.R. et al. (1999)

The egg and the chicken

The 100,000-Year Ice-Age Cycle Identified and Found to Lag Temperature, Carbon Dioxide, and Orbital Eccentricity

Nicholas J. Shackleton

The deep-sea sediment oxygen isotopic composition ($\delta^{18}O$) record is dominated by a 100,000-year cyclicity that is universally interpreted as the main ice-age rhythm. Here, the ice volume component of this $\delta^{18}O$ signal was extracted by using the record of $\delta^{18}O$ in atmospheric oxygen trapped in Antarctic ice at Vostok, precisely orbitally tuned. The benthic marine $\delta^{18}O$ record is heavily contaminated by the effect of deep-water temperature variability, but by using the Vostok record, the $\delta^{18}O$ signals of ice volume, deep-water temperature, and additional processes affecting air $\delta^{18}O$ (that is, a varying Dole effect) were separated. At the 100,000-year period, atmospheric carbon dioxide, Vostok air temperature, and deep-water temperature are in phase with orbital eccentricity, whereas ice volume lags these three variables. Hence, the 100,000-year cycle does not arise from ice sheet dynamics; instead, it is probably the response of the global carbon cycle that generates the eccentricity signal by causing changes in atmospheric carbon dioxide concentration.

Shackleton, N., 2000, Science, 289, 1897-1902.

The egg and the chicken (2)

Fig. 5. Linear variance spectra obtained by cross-spectral analysis versus ETP (25) of (A) deep-Pacific temperature, (B) ocean $\delta^{18}O$ (ice volume, sea level), (C) Vostok D/H (Antarctic air temperature), and (D) Vostok atmospheric CO_2. In each panel, the top section shows the amplitude and (shaded area) coherent amplitude spectrum, and the bottom shows phases (with 95% confidence limits) for each orbital band (using the convention where a positive phase angle is a measure of the lag in degrees with reference to ETP, that is, with reference to insolation in the Northern Hemisphere midsummer). Arrows labeled "e," "t," and "p" identify the frequencies associated with eccentricity, obliquity (tilt), and precession. The bar labeled "BW" indicates the bandwidth.

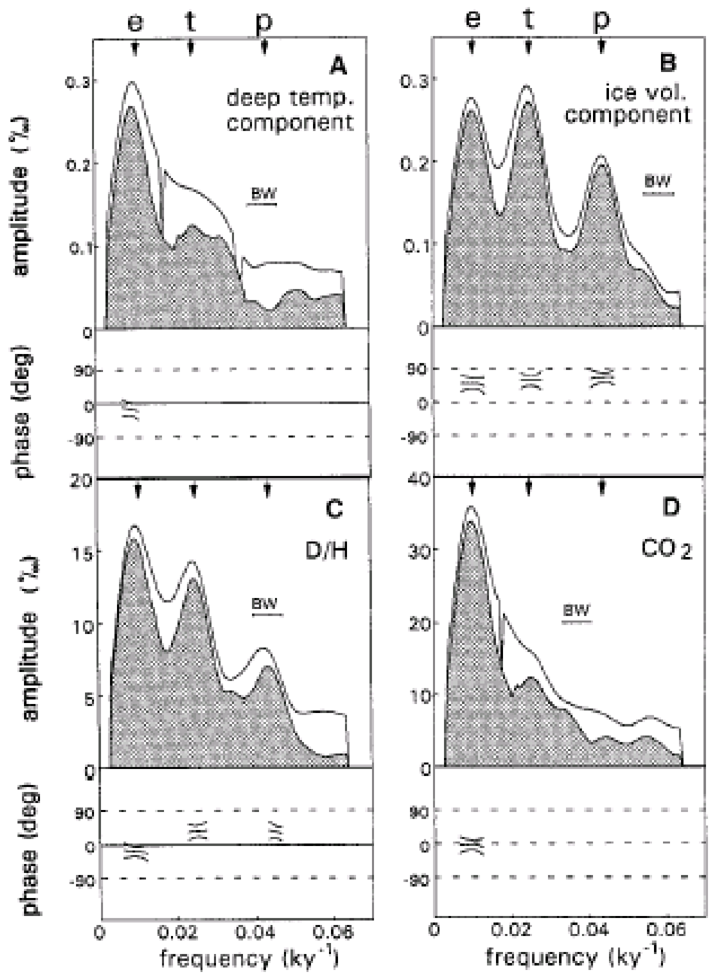

25. ETP [see (9)] denotes a convenient artificial mix of orbital eccentricity, tilt (obliquity), and precession signals with more or less equal variance and with the phase of midsummer Northern Hemisphere insolation. In view of the shortness of the records considered here, as well as the fact that none of the records under discussion display much low-frequency variance, I have removed the low frequency (400-ky period) of orbital eccentricity variability in constructing the version of ETP used.

9. J. Imbrie *et al.*, in *Milankovitch and Climate*, A. Berger *et al.*, Eds. (Reidel, Hingham, MA, 1984), pp. 269–305.

Shackleton (2000)

How well do we understand ice age cycles?

Partly based on ideas by Imbrie et al. (1984) and Imbrie et al. (1992), Saltzmann (2002) proposed a dynamical model of the northern hemisphere ice-sheet and bedrock evolution and concomitant CO_2 and ocean state variations.

The model can account for the main system transitions during the last 5 Myr. The model is forced only by: (i) variations in insolation of the NH high latitudes; (ii) slow variations of CO_2 due to tectonic processes. It includes fast- and slow-response variables, and allows for internal instabilities.

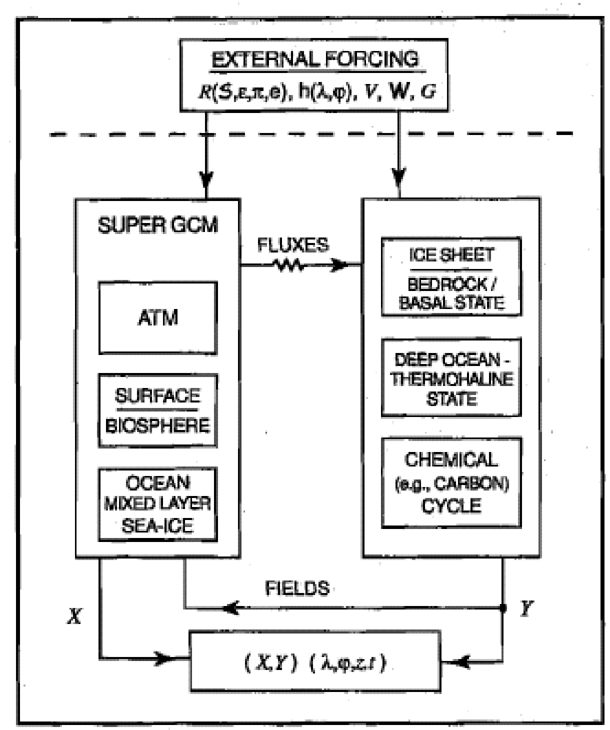

Figure 5-3 Schematic representation of the relationships between external forcing, the fast-response variables (X), and the slow-response variables (Y), showing the central role of a paleoclimatic dynamics model governing the global mean variables ($\hat{Y}$).

Saltzman (2002).

Internal instabilities

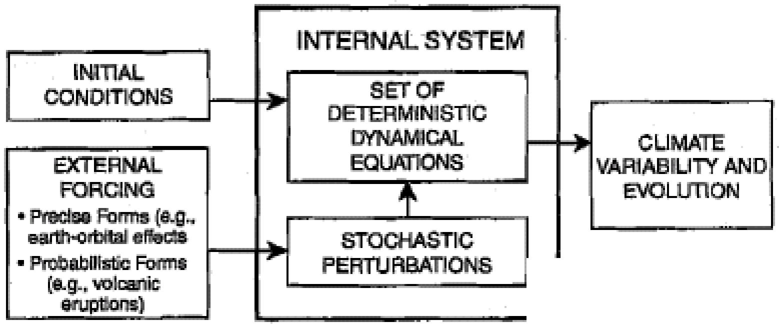

Figure 6-17 Schematic flowchart, showing the components of a including stochastic effects.

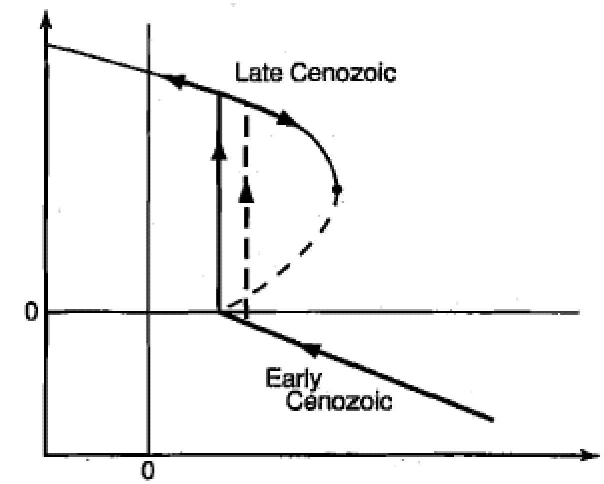

Figure 13-10 Possible path of the equilibrium state of the thermohaline state of the ocean $(\widehat{\psi}_{max}, \widehat{S}_p)$ from the Early to Late Cenozoic as a function of the forcing function $\Pi(\widehat{\mu}_G, h)$ based on the two-box model bifurcation diagram shown in Fig. 11-5.

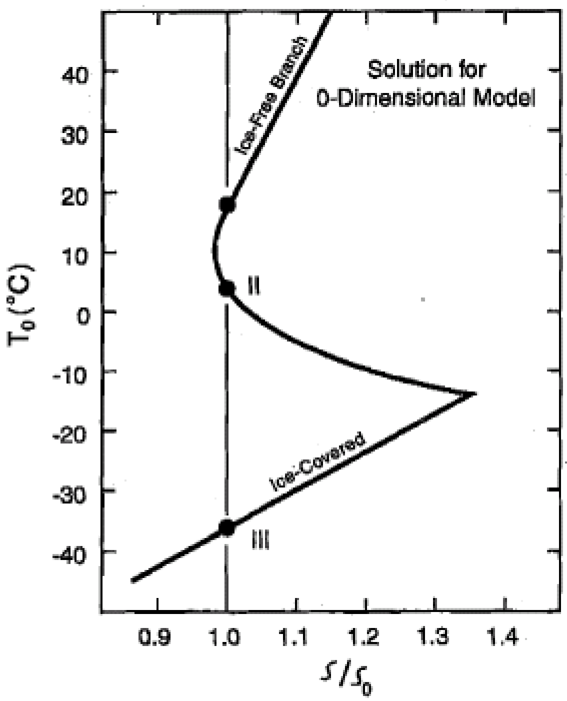

Figure 7-3 Steady-state temperatures corresponding to the climate solutions for a zero-dimensional climate model with variable ice cap as a function of solar constant in units of its present value. The roots (I, II, and III) correspond to the solutions for the present level of solar forcing. After North *et al.* (1981).

Saltzman (2002).

Geochemical processes affecting atm. CO_2

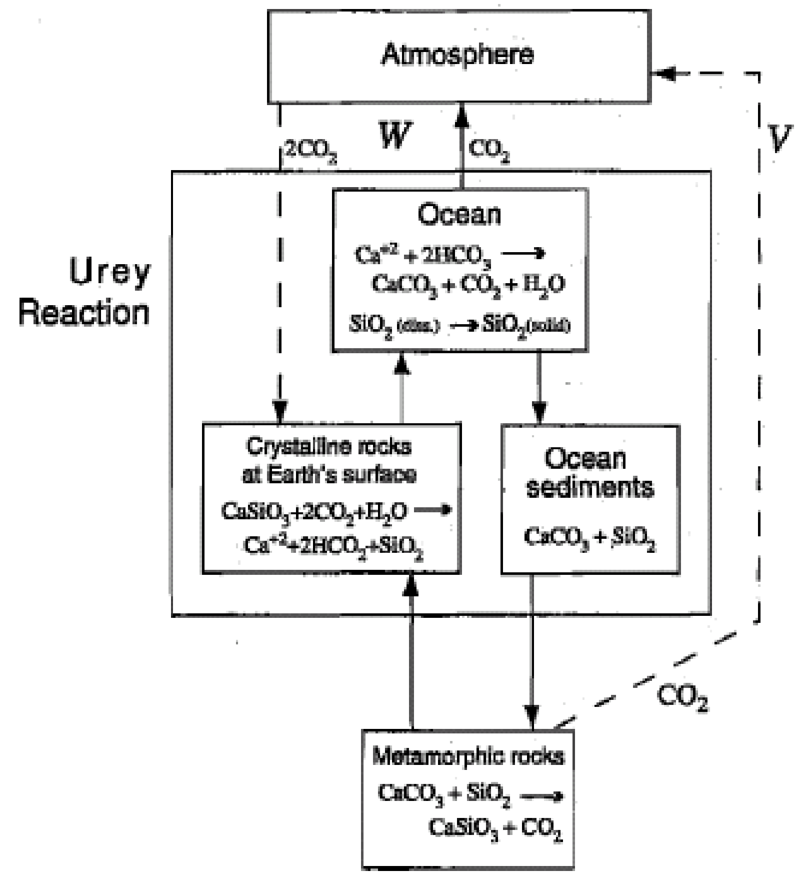

Figure 10-6 Schematic representation of the main geochemical links and reactions that determine the atmospheric CO_2 concentration on a time scale greater than 1 My. After Sarmiento and Bender (1994).

Saltzman (2002).

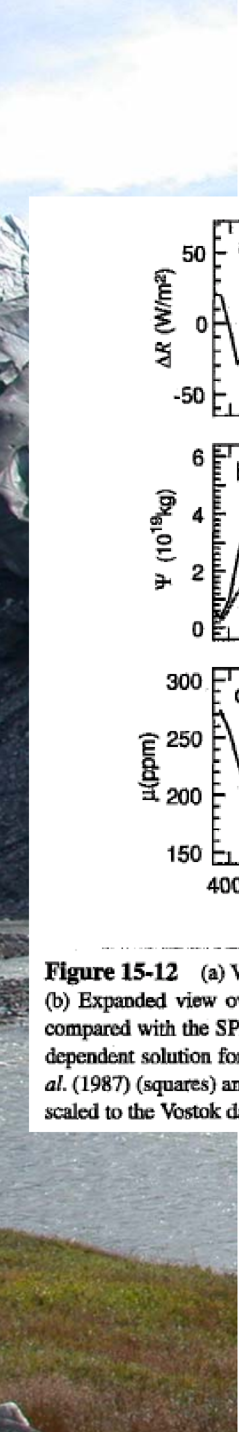

Some results

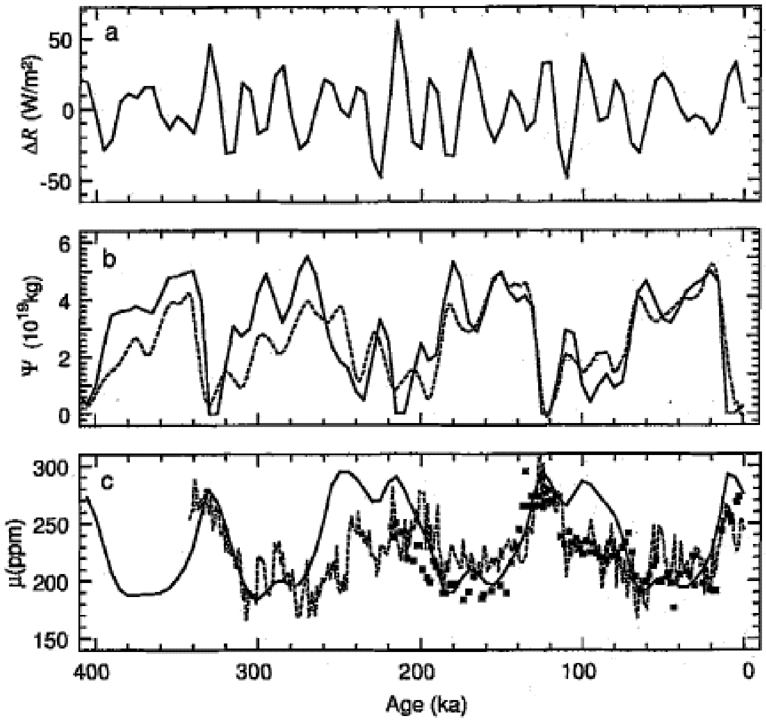

Figure 15-12 (a) Variations of July insolation at 70°N due to Earth-orbital forcing over the past 400 ky. (b) Expanded view over the past 400 ky of the time-dependent solution for ice mass, Ψ (solid curve), compared with the SPECMAP $\delta^{18}O$ reconstruction, scaled in terms of ice mass (dashed curve). (c) Time-dependent solution for total carbon dioxide μ (solid curve), compared with Vostok CO_2 data of Barnola *et al.* (1987) (squares) and the Shackleton and Pisias (1985) $\delta^{13}C$ estimates of CO_2 (dashed curve), which are scaled to the Vostok data.

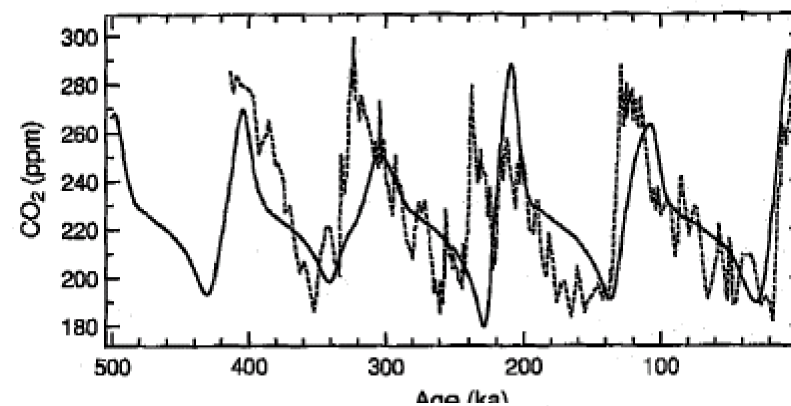

Figure 15-14 Comparison of the CO_2 solution obtained by Saltzman and Maasch (1990) (solid curve), with the Vostok CO_2 measurements going back 420 ky (Petit *et al.*, 1999) (dashed curve).

Saltzman (2002).

How well do we understand ice age cycles? (2)

The sequence of processes implied by the model is as follows:

- Tectonic forcing → long-term variations in CO_2, with low values over the Pleistocene, favouring cold T and ice formation;
- At low enough CO_2 → ice formation over NH, linearly influenced by earth-orbital variations near 20- and 40-kyr-time scales (Milankovitch);
- Slow growth of NH ice sheets → reduction of sea level, enhanced cold deep water production and shallowing of the thermocline;
- At a critical stage → activation of positive feedbacks inherent in oceanic CO_2 pumping → reduction CO_2 partial pressure in the ocean surface layer and consequently in the atmosphere. A new quasi-equilibrated state is achieved with low CO_2, large ice sheets and a cold ocean;
- Shallow thermocline and relatively strong thermohaline circulation → net leakage of CO_2 back to the atmosphere → increase in atm. CO_2 concentrations → enhanced greenhouse → surface warming and ice sheet melt;
- slow rise in atm. CO_2 → general warming and deactivation of CO_2 pumps → sharp increase in atm. CO_2 → termination of main ice age. At the same time deepening of the thermocline begins to restrict the release of CO_2 to the atmosphere → no equilibrium possible and generation of a near 100-kyr oscillation.

How well do we understand ice age cycles? (3)

Essential processes in the near 100-kyr cycle are:

- glacial state that promotes the gowth of a ‘cold-mode’ ocean with shallow thermocline;
- in this state a more symmetric thermohaline circulation → upwelling of carbon reach water → increase in atm. CO_2 conc.;
- increasing atm. CO_2 → start deglaciation;
- increase in atm. CO_2 is accentuated by positive feedbacks (warming of ocean and land masses, rise in sea level, reduction of the biological CO_2 pump in the ocean, ...);
- sharply increasing atm. CO_2 → calving and bedrock lifting → collapse of remaining ice caps → warming of ocean → establishment of a ‘more normal’ thermohaline (~ today’s state);
- ‘warm-mode’ ocean → deeper thermocline → reduced CO_2 efflux to the atmosphere → decrease in atm. CO_2;
- back to glacial state.

The chronology for this 100-kyr cyclic behavior is set by the near 100-kyr-period envelope of Milankovitch forcing, which imposes a ‘phase-lock’ on the cycle by constructive interference of the max/min in high-latitude incoming radiation of near 20- and 40-kyr periods with max/min of CO_2.

How well do we understand ice age cycles? (4)

The main conclusion of Saltzman (2002) is as follows.

‘In summary, [the model] can account for the [observed variations] by assuming that positive feedbacks in the carbon cycle can provide the instability necessary to drive a free oscillation.

As a side consequence of this theory, predictions of the longer term behavior are made that include the mechanism for the onset of the ice ages at about 2.5 Myr and the initiation of a strong near 100-kyr-period oscillation about 0.9 Myr ago.

In agreement with the conclusion expressed by Imbrie et al. (1992), it would appear that the near 20-kyr and 41-kyr-period variations are linearly forced by earth-orbital changes. However, we suggest more strongly than Imbrie et al. (1993) that the main 100-kyr-period oscillation is internally driven by an instability, probably residing in the behavior of the carbon cycle, with Milankovitch forcing playing the more secondary role of setting the phase of this oscillation.’

Again, the main cause for the onset of ice ages is the reduction of CO_2 induced by tectonic processes.

El Niño and the Southern Oscillation (ENSO) *

Probably the most famous and well-studied example of internal variability of the climate system on time scales ~10 years is the so-called ‘El Niño Southern Oscillation’ (ENSO) phenomenon (Philander, 1983).

NATURE VOL. 302 24 MARCH 1983 — REVIEW ARTICLE — 295

El Niño Southern Oscillation phenomena

S. G. H. Philander

Geophysical Fluid Dynamics Laboratory/NOAA, Princeton University, Princeton, New Jersey 08540, USA

At intervals that vary from 2 to 10 yr sea-surface temperatures and rainfall are unusually high and the tradewinds are unusually weak over the tropical Pacific Ocean. These Southern Oscillation El Niño events which devastate the ecology of the coastal zones of Ecuador and Peru, which affect the global atmospheric circulation and which can contribute to severe winters over northern America, often develop in a remarkably predictable manner. But the event which began in 1982 has not followed this pattern.

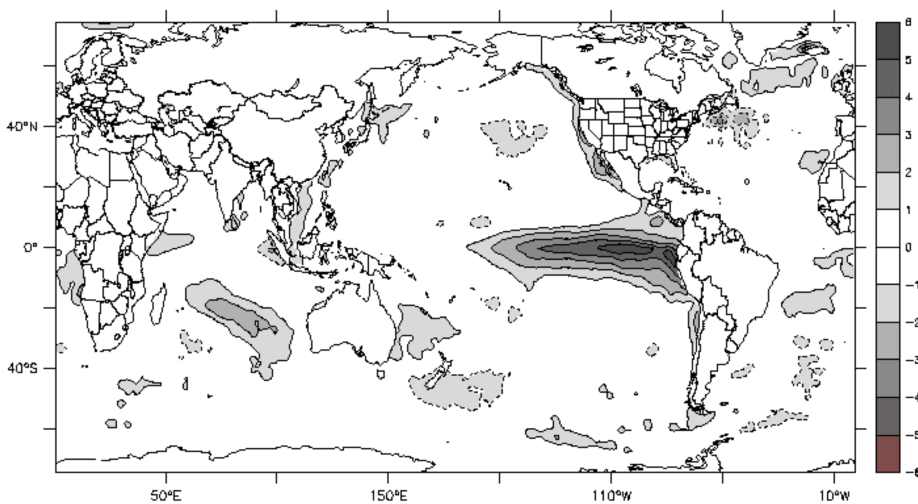

Anomaly of the sea-surface temperature in December 1997, during the 1997/1998 El Niño

* This section is partly based on material kindly provided by **C. Appenzeller**.

The name 'El Niño'

The name El Niño comes from the fact that a warm current flows southward along the coasts of Ecuador and Peru in Jan-Feb-Mar; the current means the end of the fishing season and its onset at about Christmas was the reason why the phenomenon was called by the local people El Niño ('The Child').

In some years, positive temperature anomalies are exceptionally high and persist for longer, curtailing the subsequent normal cold upwelling seasons, with distastrous consequences for the local fishers. This was for instance the case in 1982 (Philander, 1983).

Nowadays the term El Niño is associated to this more dramatic events.

Oceanic currents

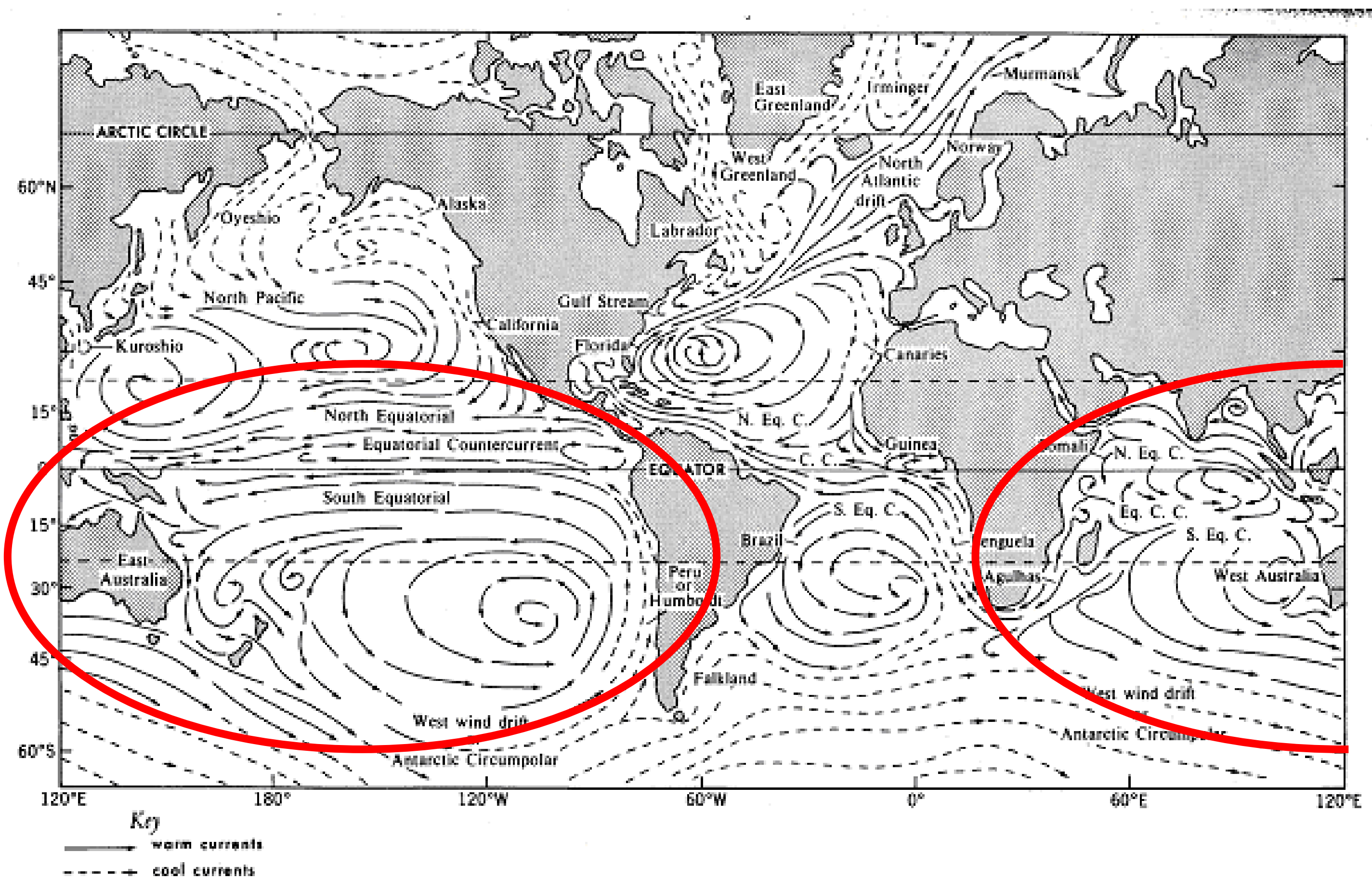

From Trenberth, K.E., 1992: *Climate System Modeling*, Cambridge University Press, Cambridge, 788 pp. (p. 123)

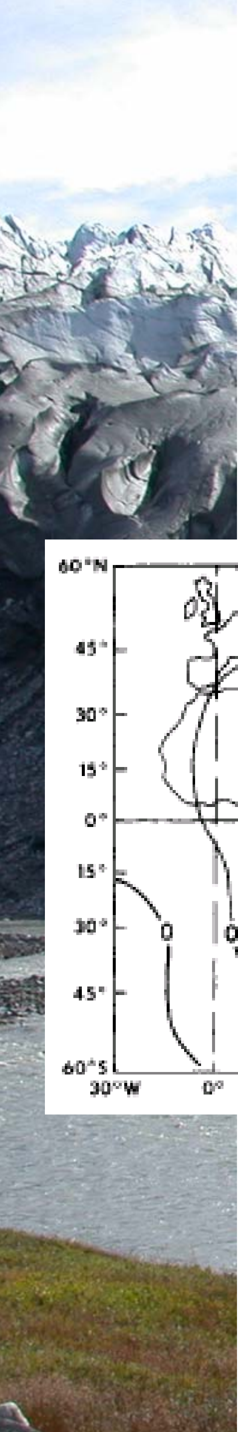

The Southern Oscillation

The discover of the Southern Oscillation is due to Sir Gilbert Walker (papers published in the 1920s and 1930s), who found that ‘when pressure is high in the Pacific Ocean, it tends to be ow in the Indian Ocean from Africa to Australia.’ The associated circulation is know called Walker circulation.

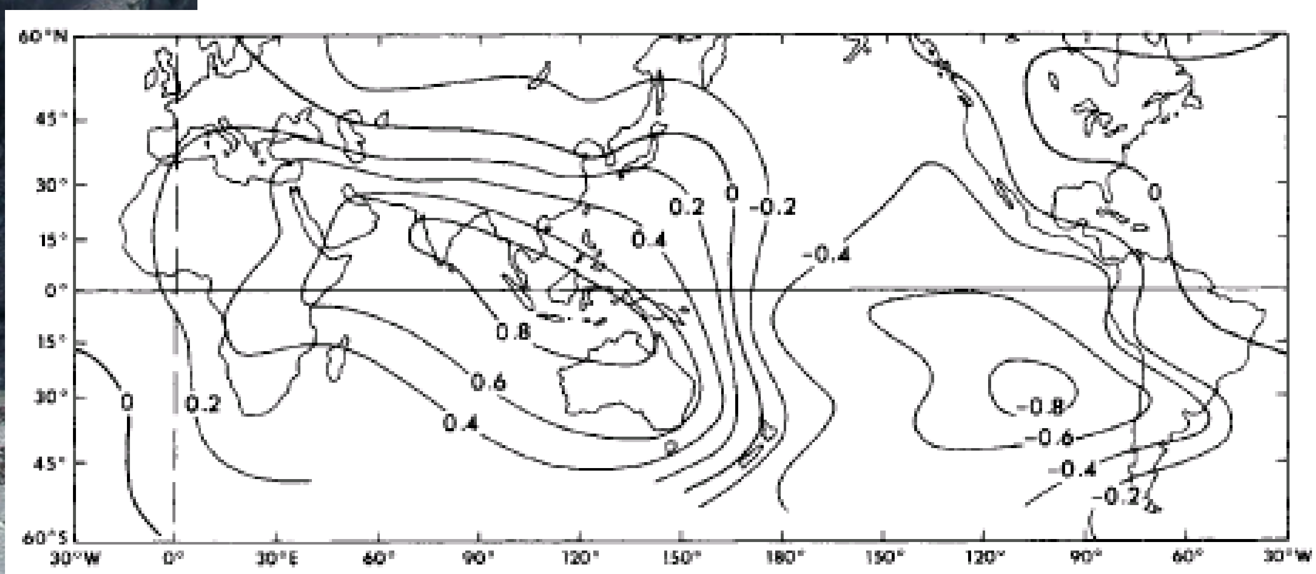

Fig. 1 The correlation of monthly mean surface pressure with that of Djakarta[45]. The correlations are large and negative in the South Pacific High Pressure Zone and are large and positive in the Australian–Indonesian Low Pressure Zone. The SO is not a standing oscillation so that correlations do not have a maximum at zero lag[46,47].

Philander (1983)

The Southern Oscillation (2)

The map shows that the SO is a barometric record of exchange of atmospheric mass along the complete circumference of the globe in tropical latitudes. Based on the pressure difference between the two centers of the previous map (Darwin and Easter Island) one can construct the so-called Southern Oscillation Index (SOI).

The standard view about periodicities in the SO is that while it has an average period of ~ 3 years, it is irregular in nature, as seen in the time series of the SOI (next page).

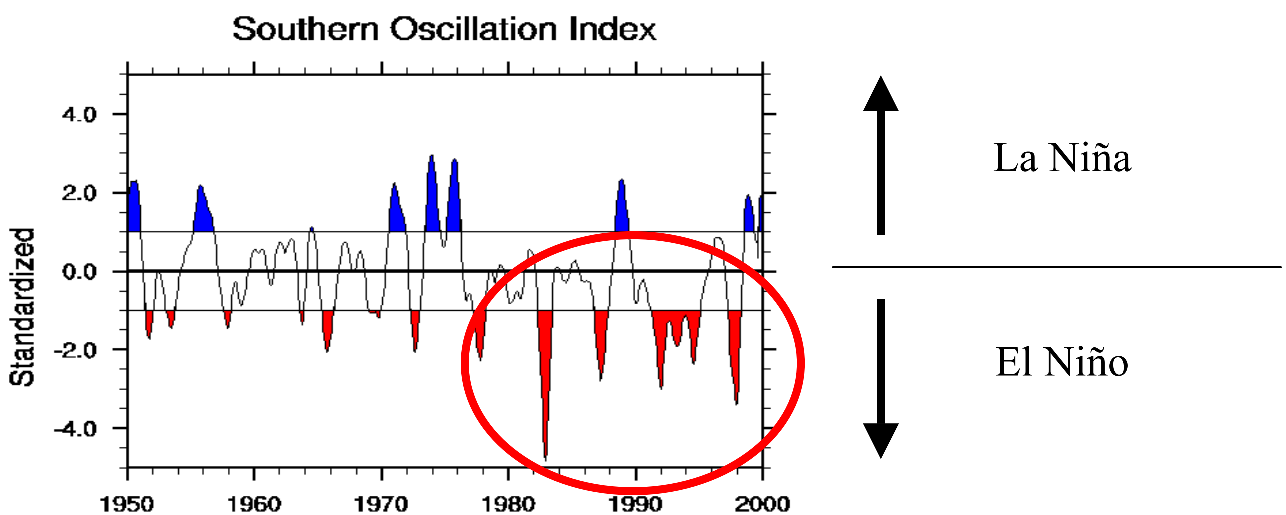

Courtesy of C. Appenzeller

Atmospheric-oceanic interactions

The links between atmospheric patterns (Southern Oscillation) and large-scale fluctuations on the surface temperature of the tropical Pacific (El Niño) are the key to ENSO.

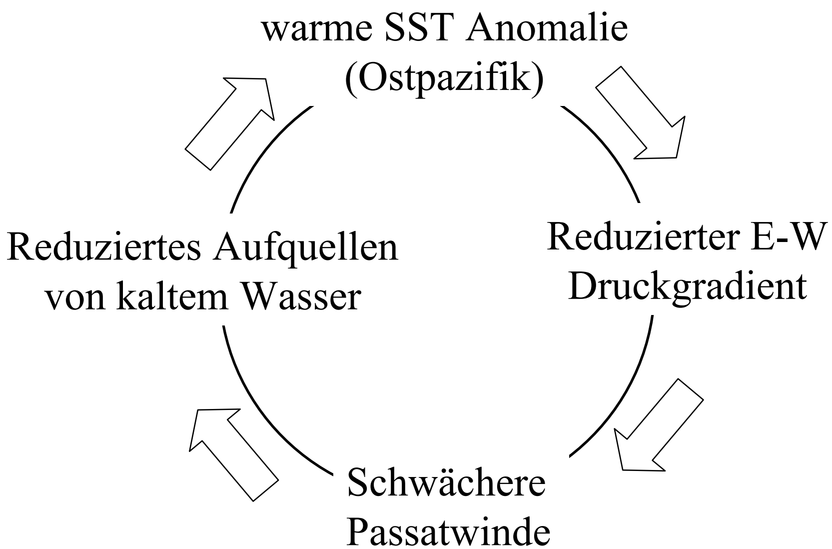

Courtesy of C. Appenzeller

Impacts of El Niño

The following figures shows the impact of the 1997/98 El Niño.

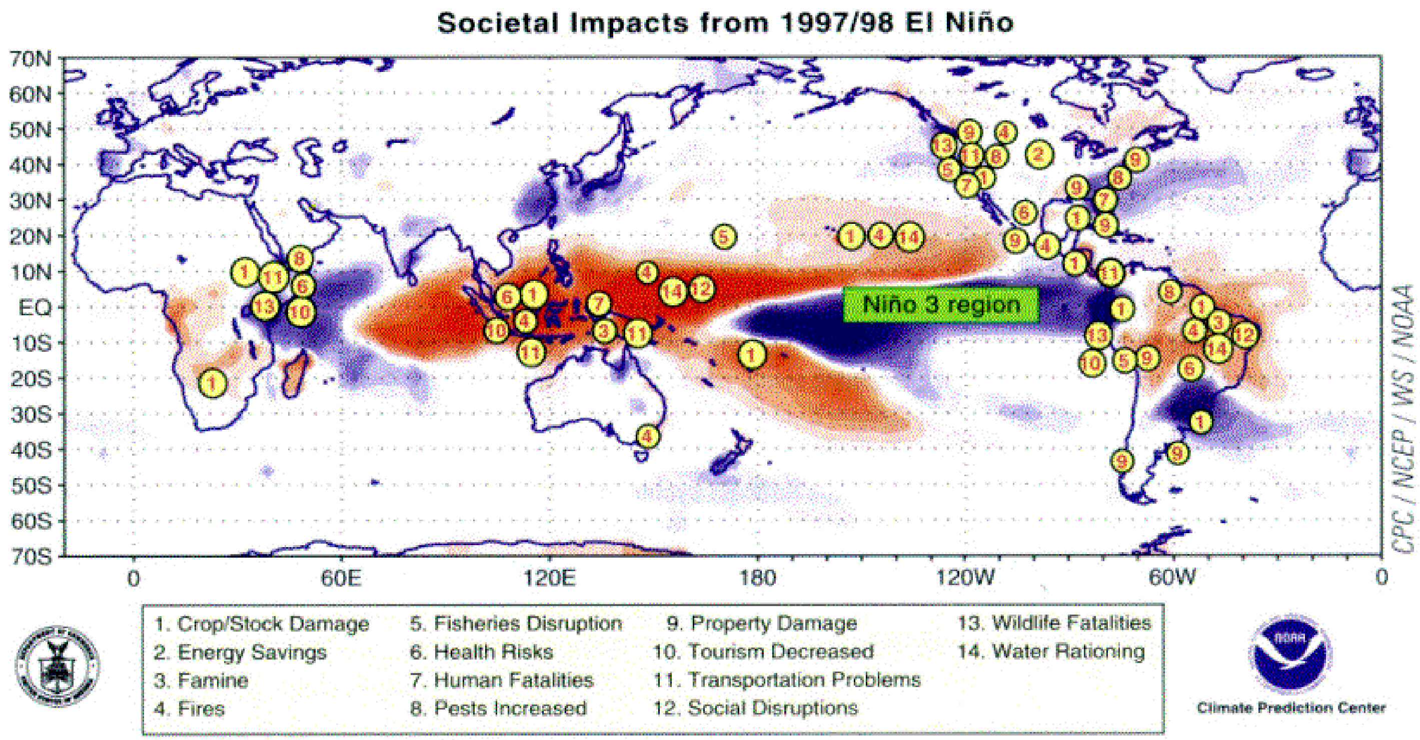

Red: rainfall below normal, blue: rainfall above normal. Compare the observed rainfall pattern with that predicted by the coupled ocean-atmosphere model; see page 23.

Courtesy of NOAA (Climate Prediction Center)

A typical El Niño

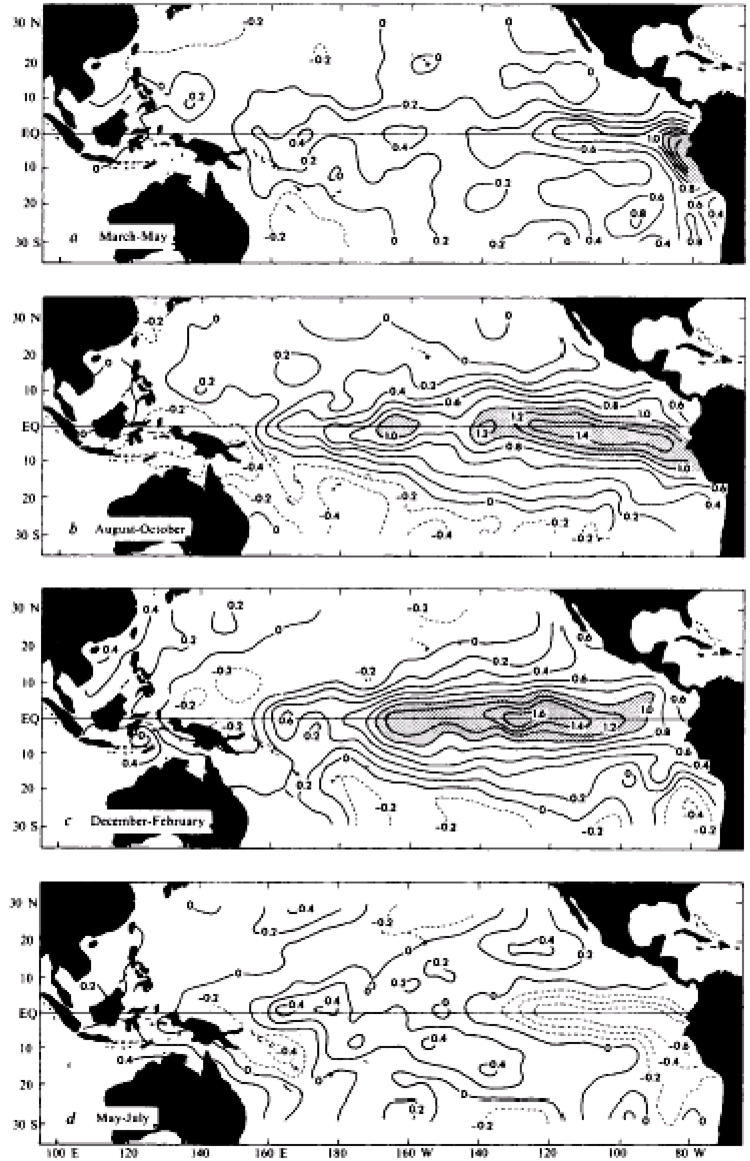

Fig. 3 Sea-surface temperature anomalies (in °C) during a typical ENSO event obtained by averaging data for the events between 1950 and 1973. *a*, March, April and May after the onset; *b*, the following August, September and October; *c*, the following December, January and February; *d*, May, June and July, more than a year after the onset[12].

Philander (1983)

A sequence of events

The events associated to a typical El Niño are:

- prior to the onset of a El Niño changes in the large scale atmospheric circulation patterns, with an increase in pressure over the western Pacific and associated weakening of the trade winds west of the dateline.
- shift of the ITCZ toward the south;
- during the mature phase, westward expansion of anomalous conditions. very weak trade winds. This phase is highly predictable;
- besides changes in the atmosphere, changes in the oceanic settings occur. Due to very weak trade winds, sea level in the western Pacific falls and the depth of the thermocline is reduced;
- intense eastwards oceanic currents between the equator and 10 ^{o}N carry warm waters away from the west Pacific (this is the reason for the apparent westward propagation of the positive sea surface temperature anomaly);
- along the western coast of the Americas there is an increase in sea level that propagates polewards in both hemispheres. This motion creates an eastward propagating Kelvin wave;
- return to normal conditions: the amplitude of the anomalous conditions off the coast of South America returns to normality a few months after the onset of El Niño.

El Niño and the global atmosphere

The anomalies associated to ENSO can be felt outside the tropics. We speak of <u>teleconnections</u> with extratropical latitudes.

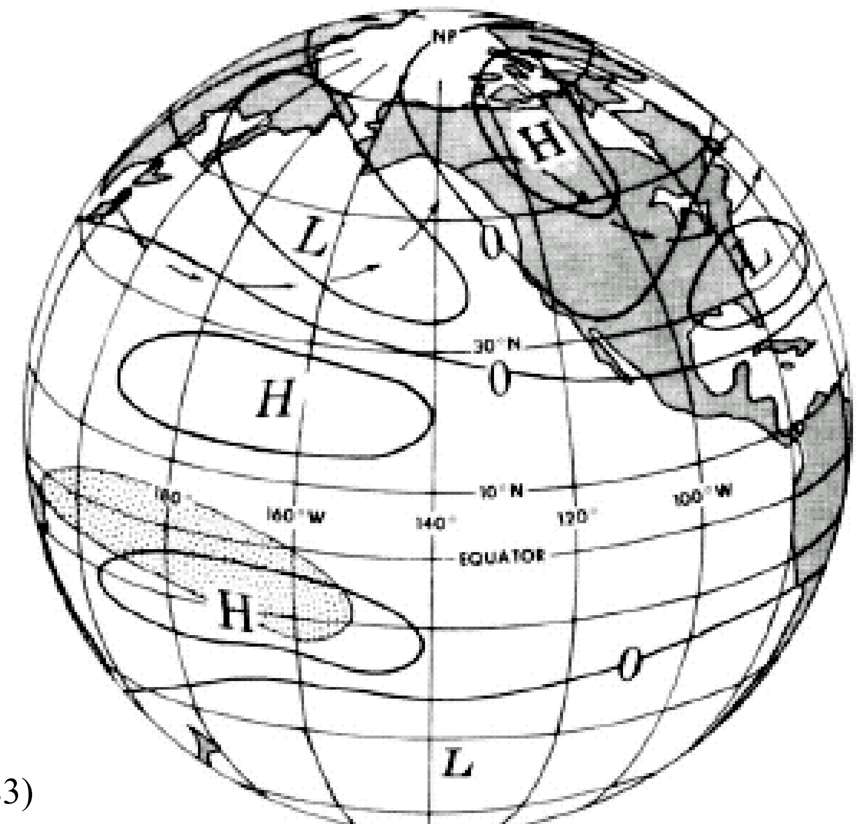

Philander (1983)

Fig. 7 Teleconnections to the extratropics during ENSO.

El Niño and La Niña revisited

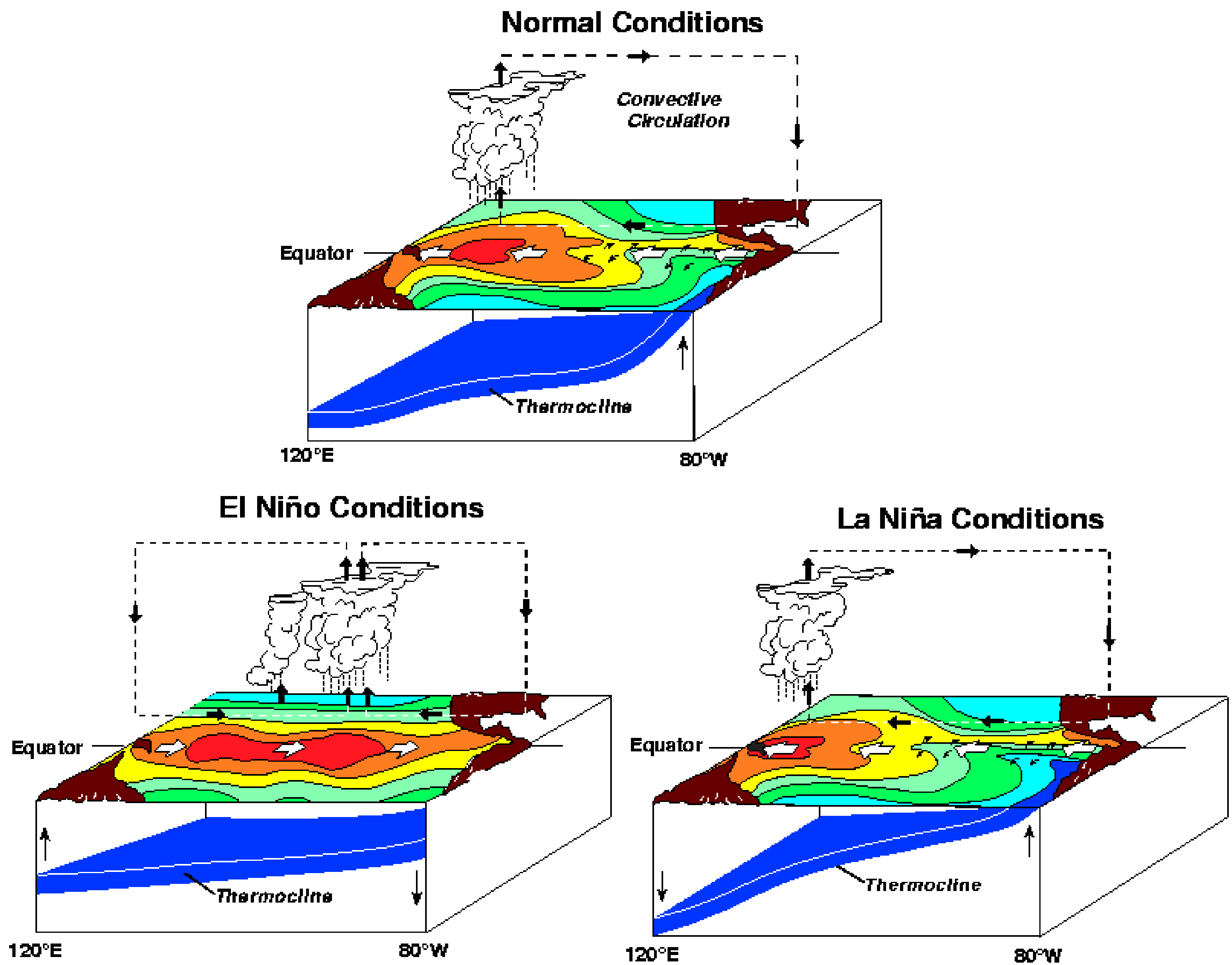

Calanca, 21.06.2006

ENSO on the web

Two very useful addresses are those of:

- The ‘Tropical Atmosphere Ocean project’ (TAO)
  http://www.pmel.noaa.gov/tao/

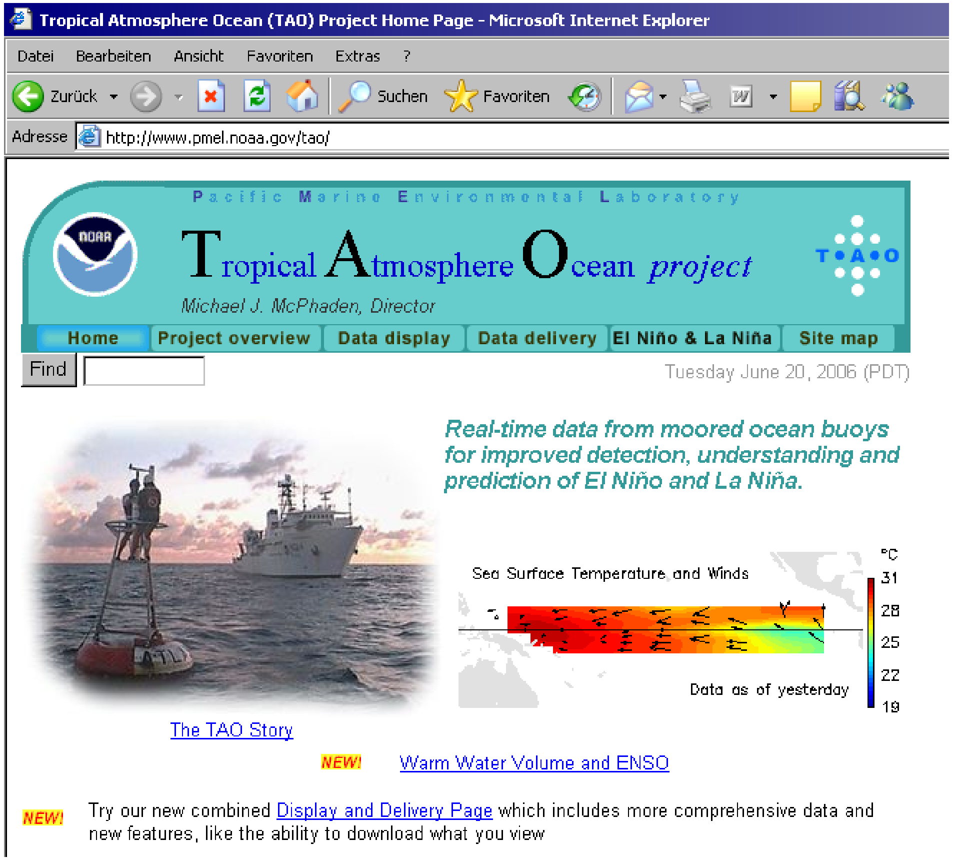

ENSO on the web (2)

- The National Oceanic and Atmospheric Administration (NOAA) http://www.elnino.noaa.gov/

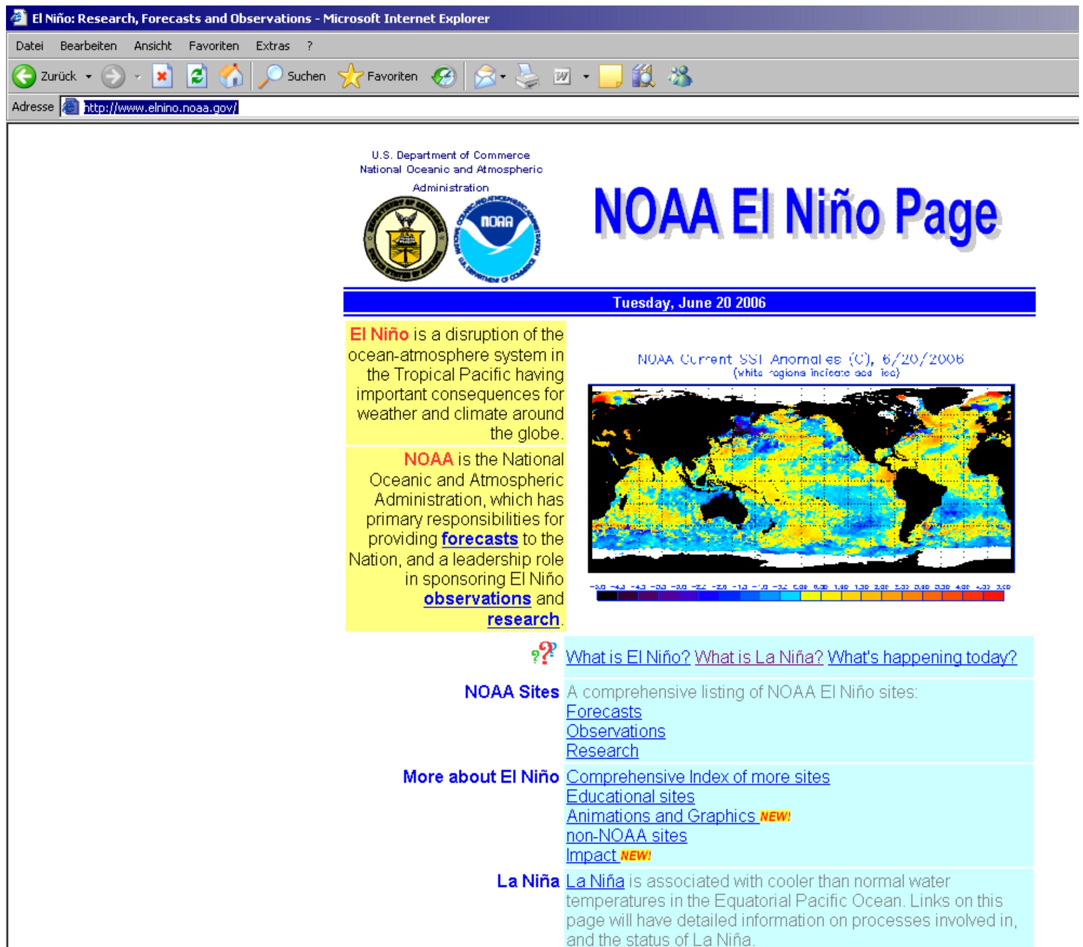

ENSO on the web (3)

- NOAA-TAO
  http://www.pmel.noaa.gov/tao/elnino/nino-home.html